Original Article

Institution of MECHANICAL ENGINEERS

Journal of SYSTEMS AND CONTROL ENGINEERING

Proc IMechE Part I:
J Systems and Control Engineering
2019, Vol. 233(5) 491–500

DOI: 10.1177/0959651818802088
journals.sagepub.com/home/pii
SAGE

Orbitally stabilizing control for the underactuated translational oscillator with rotational actuator system: Design and experimentation

Chuande Liu[1], Bingtuan Gao[1], Jianguo Zhao[2] and Syed Awais Ali Shah[1]

Abstract

Underactuated translational oscillator with rotational actuator systems are simplified mechatronic systems introduced to investigate the despin maneuver phenomenon for dual-spin spacecrafts in mechanical engineering. The conventional research work for translational oscillator with rotational actuator systems mainly focuses on stabilizing control of equilibrium points. In this article, an orbitally stabilizing control strategy is proposed to steer oscillating movements of a translational oscillator with rotational actuator system. Based on the natural periodicity of translational oscillator with rotational actuator system self-sustained oscillation, the dynamics is analyzed to derive the periodically orbital functions of the translational oscillator with rotational actuator system. Then, a proper control Lyapunov function following the principle of energy conservation is designed to obtain orbitally stabilizing controller for target periodical oscillation orbits of the translational oscillator with rotational actuator system. Finally, the validity of the presented control strategy is demonstrated via the simulations and experiments.

Keywords

Translational oscillator with rotational actuator, orbit planning, Lyapunov methods, friction compensation, orbit tracking

Date received: 12 April 2018; accepted: 24 August 2018

Introduction

Underactuated mechanical systems (UMS) are a class of control systems which have less control inputs than the number of configuration variables.[1] The translational oscillator with rotational actuator (TORA) or RTAC (Rotational Translational Actuator) is a benchmark of UMS, consisting of an unactuated translational oscillation cart and an actuated rotating actuator, which is originated from a simplified model of a dual-spin spacecraft and initially introduced mainly by Bupp et al.[2] For exhibiting nonlinear interaction between translational and rotational movements, the dynamical characteristics of TORA systems have been paid widely attention during the past decades,[3–6] and the control problem for TORA systems present many theoretical challenges and deserve further investigations.

Conventionally, the control objective of many ambitious works about TORA system is to realize semi-global or global stabilization of static equilibrium points.[7,8] Namely, the control objective is to employ the control input acting or the actuator to stabilize both the translational position of the unactuated oscillating cart and the rotational position of actuated rotating actuator. Inversely, how about employing the control input acting to force the translational cart to oscillate periodically or track the desired orbits in state space of the TORA system? Compared with the two inverse control objectives, any static equilibrium point of the TORA system is quite analogous to the special periodic orbit of the forcing stable oscillations, that is, the period of the oscillation orbit is zero. Consequently, stabilizing control of equilibrium points can be seen as orbitally stabilizing control of the special target periodic orbits. In practice, the orbitally stabilizing control of the TORA systems, similar to that of other UMS,[9–13] is to

[1]School of Electrical Engineering, Southeast University, Nanjing, P.R. China
[2]Department of Mechanical Engineering, Colorado State University, Fort Collins, CO, USA

Corresponding author:
Bingtuan Gao, School of Electrical Engineering, Southeast University, No. 2 Sipailou, Nanjing 210096, P.R. China.
Email: gaobingtuan@seu.edu.cn

force their degrees of freedom (DOFs) to track some periodic oscillating orbits in state space, which is harder to achieve but has promising application prospects.

Although the problem of forcing oscillations in many other practical application systems which present analogous working principles, for example, tuned mass damper,[14] vibrating screens,[15] and vibration conveyors[16], is a classical area of research, orbitally stabilizing control in UMS is mainly focused on theoretical developments or based on simulations,[17,18] which remains underexplored. For benchmarks of UMS,[19,20] the major difficulty of the orbitally stabilizing control compared with the stabilizing control of equilibrium points is orbit planning and orbit tracking control design. As early as in 1995, Chung and Hauser[21] studied stabilizing controller of dynamic orbit for a pendulum-like UMS. Then, Shiriaev et al.[22] presented a tool based on systematic virtual constraints for generation and orbital stabilization of periodic orbits, which could be applied to several pendulum-like UMS.[23] Aiming at benchmarks of UMS with one underactuated DOF, Gao et al.[24] also employed the orbitally stabilizing controller based on virtual constraints to TORA system successfully. However, for the orbitally stabilizing control based on virtual constraints technique, its physical meaning is actually ambiguous and the design procedure is relatively complicated.

In physical platform, with the TORA dynamic movements, matched external frictional effects are unavoidably encountered, and unless dealt with the problems in a proper way, they would lead to mission failure such as deteriorating the performances of the control methods and giving rise to unstable results. In the above works on TORA system, the stabilizing control strategies of equilibrium points were validated by experimental results;[4,5] however, most of orbitally stabilizing control strategies were based on simulations.[21–24]

In this article, following our previous work,[24] the novel periodic orbits of TORA system are proposed, which are the natural extension to the equilibrium points. Comparing with our previous work on the periodic orbits of TORA system to steer the translational cart oscillating synchronously with the eccentric rotational actuator,[24] this article presents new periodic orbits of TORA system to force the translational oscillation cart oscillating periodically while the eccentric rotational actuator being stabilized. Then, a concise orbitally stabilizing controller is designed to track effectively the proposed periodic orbits. Specifically, target periodic orbits of the TORA system are derived by analyzing the dynamics directly, and then a control Lyapunov function including system energy is followed to obtain a stabilizing controller for the derived periodic orbits. Finally, simulation and experimental results demonstrate the feasibility and efficiency of the presented orbitally stabilizing control. Moreover, to the best of our knowledge, it is the first method validation through experimental results on TORA platform for oscillating orbit stabilizing control.

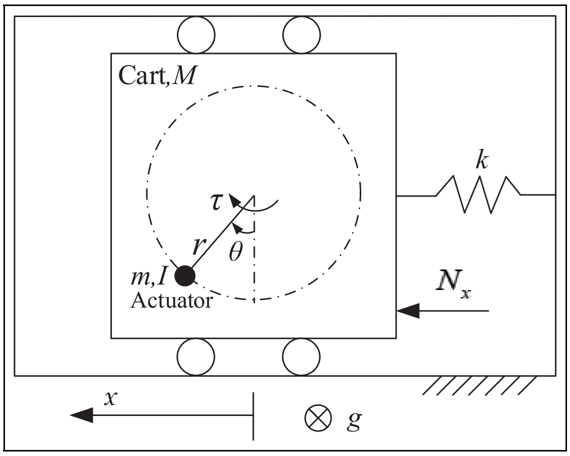

Figure 1. TORA system configuration.

A successfully orbitally stabilizing control of the TORA system demonstrates the possibility of forcing the translational cart to oscillate with one actuated rotation motion. This is an important inherent characteristic of the TORA system which has potential applications to the active vibration control of vibrating screens in coal processing.[15,25] It is well known that the vibrating screen has the performance to select different materials based on tracking the different vibration amplitudes and orbits. One of the disadvantages of classical vibration control for vibrating screens is the cost since a full-actuation or an even redundant-actuation control system is needed.[26] However, based on the characteristic of the TORA system, only one actuation is needed to control the vibration. Therefore, the idea of orbitally stabilizing controlling the TORA system could be applied to active vibration control of vibrating screens with a low cost.

In the next section, the dynamics of TORA system and target periodic orbits are described. The following section provides the design of the orbitally stabilizing controller with friction compensation. The fourth section presents some discussions of the simulations and experiments on the designed orbitally stabilizing controller. The conclusion of this article is summarized in the final section.

Dynamics and target orbits

In this section, we first present the dynamics for TORA system and then design the target orbits.

System dynamics

The TORA system is depicted in Figure 1. The inner cart having mass M is connected to an outer fixed wall by a linear spring of stiffness k. The inner cart is constrained to have one-dimensional translational movement along x-direction. The eccentric rotational actuator having mass m is attached to the cart and moment of inertia I about its center of mass, and the eccentric distance of the actuator is r. Control input torque applied to the actuator is denoted as τ. The dynamics of TORA system can be derived as follows[2]

$$(M+m)\ddot{x} + mr\cos\theta\ddot{\theta} - mr\sin\theta\dot{\theta}^2 + kx + N_x = 0 \tag{1}$$

$$mr\cos\theta\ddot{x} + \left(mr^2 + I\right)\ddot{\theta} = \tau \tag{2}$$

where x, $\dot{x}$, and $\ddot{x}$ denote the translational position, velocity, and acceleration of the cart, respectively; θ, $\dot{\theta}$, and $\ddot{\theta}$ denote the angular position, angular velocity, and angular acceleration of the eccentric rotational actuator, respectively; g denotes the gravity constant; and N_x denotes the disturbance acting on the translational cart.

The kinetic energy of the TORA system is calculated as follows[8]

$$K = \frac{1}{2}(M+m)\dot{x}^2 + mr\cos\theta\dot{x}\dot{\theta} + \frac{1}{2}\left(mr^2 + I\right)\dot{\theta}^2 \tag{3}$$

where K is always positive. The potential energy of the eccentric rotational actuator is $(1/2)kx^2$. Hence, the total energy (including kinetic energy and potential energy) of the TORA system is given as follows

$$E = K + \frac{1}{2}kx^2 \tag{4}$$

By neglecting the disturbance force N_x and differentiating total energy of the system E, together with the system dynamics (equations (1) and (2)), we have the following

$$\dot{E} = \tau\dot{\theta} \tag{5}$$

Integrating both sides of the above equation (5) we have the following

$$\int_0^t \tau\dot{\theta}(t)dt = E(t) - E(0) \geqslant -E(0) \tag{6}$$

A system is passive if it has a positive semi-definite storage function $S(\xi)$ and a bilinear supply rate $\omega(u,y) = u^T y$, satisfying $\int_0^\kappa \omega(u(t),y(t))dt \geqslant S(\xi(\kappa)) - S(\xi(0))$ for the input u, the output y, and $\kappa \geqslant 0$.[27] In equation (6), $E(t)$ can be seen as storage function $S(\xi)$; therefore, the TORA system having τ as input and $\dot{\theta}$ as output is passive. This passivity property of the system dynamics is a key character of UMS since a passive UMS has a stable origin and a feedback control law always exists for $\dot{E} < 0$, and will be used in control design part by including system energy item into the control Lyapunov function.

Target orbit design

Note that the the angular position θ is actuated variable in the TORA system, which can be controlled directly by the control input torque τ. However, the translational position x, which is an unactuated DOF, must be controlled through coupling interaction. In other words, the nonlinear coupling interaction between the angular position of the actuator and translational position of the cart provides the basis for the control objective of TORA system. Based on this, it is straightforward that by fixing the angular position θ and letting the control input torque τ be zero in equations (1) and (2), TORA system is degraded to a simple mass–spring system whose oscillation period is calculated as follows

$$T = 2\pi\sqrt{\frac{(M+m)}{k}} \tag{7}$$

This periodic oscillating phenomenon with clear physical meaning motivates us to select the target orbit of translational cart in the form of sine function as follows

$$x_d(t) = x_0 + x_A\sin\left(\frac{2\pi}{T}t + \varphi\right) \tag{8}$$

where x_0 and φ denote the different initial position and initial phase, respectively; x_A denotes the amplitude of periodic orbit. Meanwhile, the target orbit of the eccentric rotational actuator can be selected in the form of some constant as follows

$$\theta_d = (n + \alpha)\pi \tag{9}$$

where α denotes the target physical angular position, $\alpha \in (0,1)$, and $n = 0, \pm 1, \pm 2, \ldots$.

Once the system states x and θ are steered by a proper control input torque to the given amplitude x_A and the given orbit (equation (9)) from initial conditions, that is, oscillation period T is unchangeable but the amplitude x_A is only controllable item in periodic orbit (equation (8)), the target total energy E_d of the TORA system will be fixed like a simple mass–spring system, which can be written in the form of spring potential energy as follows

$$E_d = \frac{1}{2}kx_A^2 \tag{10}$$

Remark 1. Once we let $x_0 = x_A = 0$ in equation (8), which means $x_d(t) = 0$, the designed periodic orbit of translational cart can shrink to the static equilibrium point. However, the arbitrary θ_d can be seen as the static equilibrium point in equation (9) because the actuator will stabilize on the plane perpendicular to g-direction. In this case, the designed periodic orbits (equations (8) and (9)) can be simplified to the static equilibrium point.

Remark 2. Once we let $\theta_d = (n + 0.5)\pi$ in equation (9), which means the actuator is stabilized in x-direction, then, TORA system is degraded to a simple mass–spring system for no coupling interaction acting between the rotation motion and periodic oscillation of the cart. If the actuator tracks its target orbit selected as $\theta_d \neq (n + 0.5)\pi$, for example, exactly selected as $\theta_d = 2\pi$, there will need some control input torque to keep the actuator at the target orbit position.

As control objective of this article shown in Figure 2, we will illustrate the simplified translational motion and rotational motion of the TORA system if the target orbits are selected as $x_d(t)|_{(x_0=0)}$ and $\theta_d = 2\pi$. According to Figure 2(a), the initial condition is chosen as $[x, \dot{x}, \theta, \dot{\theta}]^T|_{(t=0)} = [0, 0, 0, 0]^T$. First, once the input torque τ works, based on the coupling interaction between translational and rotational movements, both the translational position of the cart and the angular position of the rotor need to be controlled. Figure 2(b) implies the fact that the cart of translational motion along x is inversely proportional to N_x. Then, we can see that the actuator is rotated at the angular position $(0 < \theta < \pi)$, while the cart is driven close to x_A by the coupling interaction to meet the law of conservation of momentum along the x-axis direction. Similarly, if the actuator is driven to the angular position $(\pi < \theta < 2\pi)$ by the input torque τ, the cart can be driven closely to $-x_A$. This can be explained according to Figure 2(c). Next, once the angular position is stabilized at 2π (also shown in Figure 2(a)), the amplitude of the cart motion reaches x_A. Meanwhile, the nonlinear coupling interaction generated from translational and rotational movements would disappear, and then the TORA system is degraded to a simple mass–spring system. Finally, if N_x is neglected in the dynamics, the cart will keep persistent oscillation; otherwise, friction compensation will be considered to track target orbits.

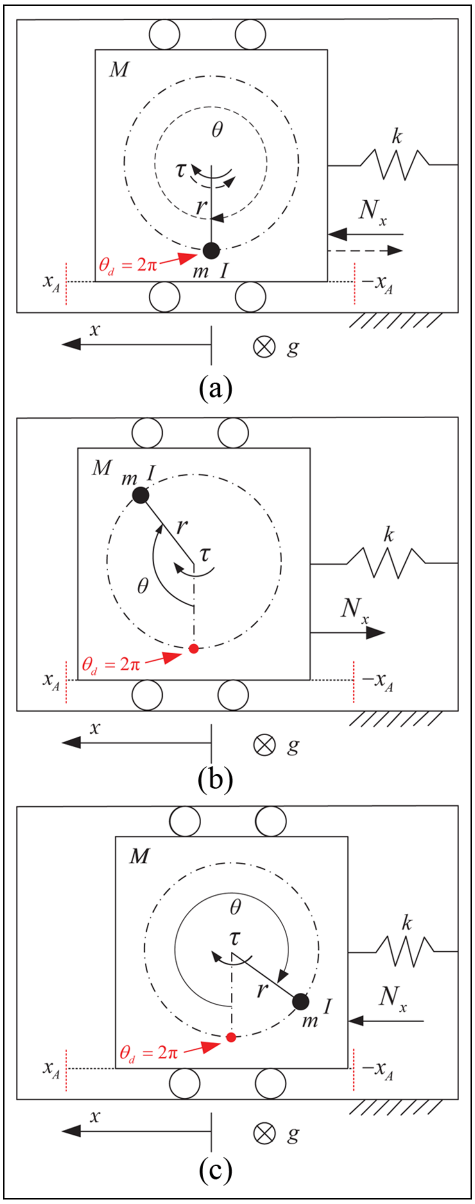

Figure 2. The tracking process of orbitally stabilizing control for TORA system from equilibrium point to the target orbits: $x_d(t) = x_A \sin((2\pi/T)t + \varphi)$, $\theta_d = 2\pi$. (a) initial conditon; (b) condition of $0 < \theta < \pi$; (c) condition of $\pi < \theta < 2 * \pi$.

Orbitally stabilizing control design and stability analysis

In this section, we first present the orbitally stabilizing control design and then provide the corresponding stability analysis based on LaSalle's Invariance Theorem. After that, to promote the proposed control design to practical TORA platform, compensation control and friction modeling identification will be introduced.

Controller design

According to passivity property of the system dynamics (equation (5)) and target periodic orbits (equations (8) and (9)), the following control Lyapunov candidate is proposed

$$V(x, \dot{x}) = \frac{1}{2}k_1 e_E^2 + \frac{1}{2}k_2 e_\theta^2 + \frac{1}{2}k_3 \dot{\theta}^2 \tag{11}$$

where k_1, k_2, and k_3 denote positive constants, and $e_E = E(t) - E_d$, $e_\theta = \theta - \theta_d$. Note that the control Lyapunov candidate $V(\boldsymbol{x}, \dot{\boldsymbol{x}})$ is positive definite function.

Differentiating equation (11), we have the following

$$\dot{V}(x, \dot{x}) = \dot{\theta}\left(k_1 e_E \tau_1 + k_2 e_\theta + k_3 \ddot{\theta}\right) \tag{12}$$

where τ_1 denotes the orbitally stabilizing controller of the TORA system. According to the second stability theorem of Lyapunov, we define the following equation

$$k_1 e_E \tau_1 + k_2 e_\theta + k_3 \ddot{\theta} \triangleq -k_4 \dot{\theta} \tag{13}$$

where k_4 denotes positive constant. Based on equations (12) and (13), we have the following

$$\dot{V}(x, \dot{x}) = -k_4 \dot{\theta}^2 \leqslant 0 \tag{14}$$

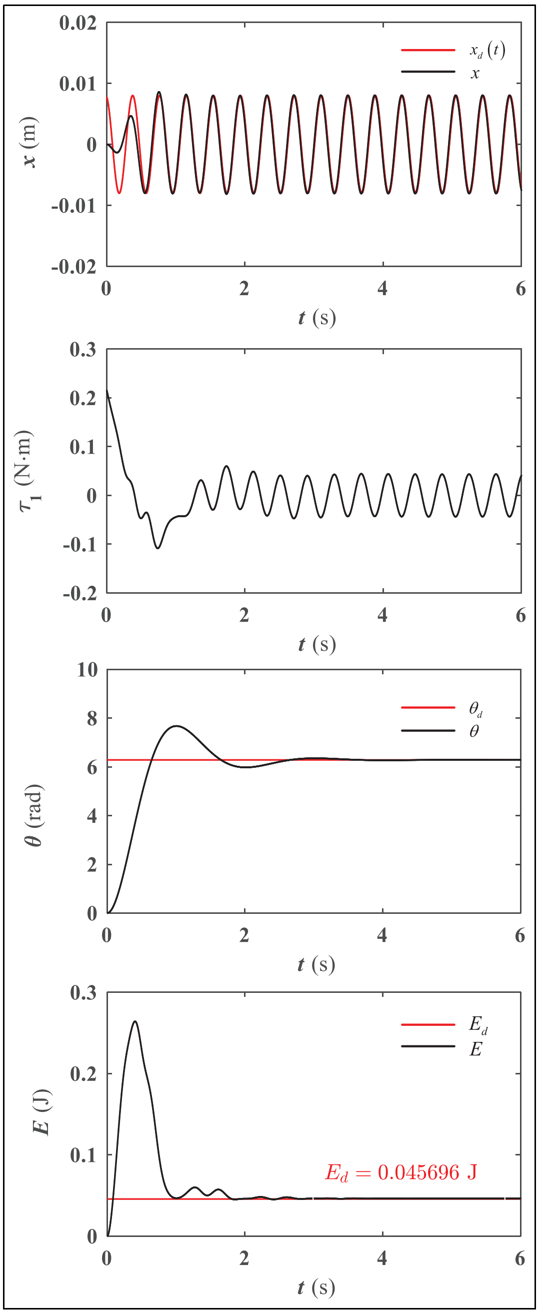

Figure 3. Simulation results of the proposed controller τ_1 for TORA system and the target orbits are chosen as $x_d(t) = 0.008\sin(16.11t + 0.57\pi)$, $\theta_d = 2\pi$.

if and only if $\dot{\theta} = 0$, $\dot{V}(\boldsymbol{x}, \dot{\boldsymbol{x}}) = 0$.

According to equation (13) and system dynamics (equations (1) and (2)), τ_1 can be calculated as follows

$$\tau_1 = -\frac{\Omega(k_4\dot{\theta} + k_2 e_\theta) + k_3 mrh_1\cos\theta}{k_1 e_E\Omega + k_3(M + m)} \tag{15}$$

where Ω denotes $(M + m)(mr^2 + I) - (mr\cos\theta)^2$ and h_1 denotes $-mr\sin\theta\dot{\theta}^2 + kx$.

In equation (15), the obtained controller τ_1 can guarantee that the time derivative of the control Lyapunov candidate is negative semi-definite. Therefore, the closed-loop control system is stable in the Lyapunov sense. To avoid the singularity, note that the denominator cannot be zero. Consequently, the control parameters k_1 and k_3 have to satisfy the following

$$\frac{k_3}{k_1} \neq -\frac{e_E\Omega}{M + m} \tag{16}$$

Remark 3. Note that e_E and Ω in equation (16) are time-varying functions, whose variation ranges are related to the orbit amplitude x_A of the cart and physical parameters of the given TORA system. Based on this, choose suitable k_1, k_3, and x_A can make sure the value of left item is always beyond the time-varying range of right item in equation (16).

To verify the feasibility and efficiency of the proposed orbitally stabilizing controller τ_1, simulations are performed as follows. First, the simulations of physical parameters are chosen the same as the TORA platform (see Figure 7): $M = 5.2\,\text{kg}$; $m = 0.3\,\text{kg}$; $I = 0.001503\,\text{kg}\,\text{m}^2$; $r = 0.0695\,\text{m}$; $k = 1428\,\text{N/m}$. Then, simulations initial state is chosen as $[x, \dot{x}, \theta, \dot{\theta}, \tau_1]^T|_{(t=0)} = [0, 0, 0, 0, 0]^T$ and followed by the chosen target orbits $x_d(t) = 0.008\sin(16.11t + 0.57\pi)$, $\theta_d = 2\pi$. Finally, the control parameters in equation (15) are tuned as $k_1 = 1$, $k_2 = 4.8$, $k_3 = 0.4$, $k_4 = 1.2$.

Figure 3 shows the simulation results of controller τ_1 driving TORA system. Note that the translational position x can basically track $x_d(t)$ and realize target periodic oscillation after 1 s for the cart. For the actuator, the angular position θ can precisely stabilize at 2π after 4 s. When both the cart and the actuator have tracked their target orbits, the total energy E will be stabilized at E_d as expected. Moreover, the value of controller τ_1 is lager than 0.2 N m at 0 s and then decrease rapidly within ± 0.05 N m. After 4 s, the controller τ_1 presents periodical changes to stabilize the eccentric rotational actuator.

Stability analysis of orbitally stabilizing controller

The stability of the closed-loop orbitally stabilizing controller is proved based on LaSalle's Invariance Theorem.

Theorem 1. For the TORA dynamics (equations (1) and (2)), the proposed orbitally stabilizing controller (equation (15)) can drive each DOF, that is, x, $\dot{x}$, θ, and $\dot{\theta}$, converging to the target periodic orbits

$$\lim_{t\to\infty}[x, \dot{x}, \theta, \dot{\theta}]^T = [x_d(t), \dot{x}_d(t), \theta_d, 0]^T$$

Proof. Based on equation (14), the time derivative of the control Lyapunov candidate, namely, $\dot{V}(\boldsymbol{x}, \dot{\boldsymbol{x}})$, is negative semi-definite. Therefore, $V(\boldsymbol{x}, \dot{\boldsymbol{x}})$ is bounded monotone decreasing function, that is, $V(\boldsymbol{x}, \dot{\boldsymbol{x}}) \in \mathcal{L}^\infty$. Then, by combining the TORA dynamics (equations (1) and (2)), each DOF in TORA system is bounded, we have the following

$$x, \dot{x}, \theta, \dot{\theta} \in \mathcal{L}^{\infty} \tag{17}$$

$$\ddot{x}, \ddot{\theta} \in \mathcal{L}^{\infty} \tag{18}$$

Substituting equations (17) and (18) into equation (15) we have the following

$$\tau \in \mathcal{L}^{\infty} \tag{19}$$

Next, let $\mathbf{\Gamma}_m$ be the largest invariant set contained in $\mathbf{\Gamma}$, which is defined as follows

$$\mathbf{\Gamma} = \left\{(x, \dot{x}, \theta, \dot{\theta}) \middle| \dot{V}(\boldsymbol{x}, \dot{\boldsymbol{x}}) = 0\right\} \tag{20}$$

According to the definition (20) and the inequality (14), $\dot{V}(\boldsymbol{x}, \dot{\boldsymbol{x}}) = 0$, if and only if $\dot{\theta} = 0$. Hence, in $\mathbf{\Gamma}$ we have the following

$$\dot{\theta} = 0 \tag{21}$$

$$\ddot{\theta} = 0 \tag{22}$$

$$\theta = \text{const} \tag{23}$$

We investigate x and $\dot{x}$ in $\mathbf{\Gamma}$. By neglecting the disturbance force N_x and substituting equation (21) into TORA dynamics (equations (1) and (2)), the input torque of TORA system can be calculated as follows

$$\tau_1 = -\frac{mr\cos\theta \cdot kx}{(M+m)} \tag{24}$$

Combining equations (15) and (21), the input torque of TORA system can also be calculated as follows

$$\tau_1 = -\frac{k_2 e_\theta \Omega + k_3 mr\cos\theta \cdot kx}{k_1 e_E \Omega + k_3(M+m)} \tag{25}$$

Obviously, based on equations (24) and (25), we have the following

$$\frac{k}{(M+m)}\frac{k_1}{k_2} mr\cos\theta \cdot e_E x = e_\theta \tag{26}$$

where we let $\theta = \text{const.} \triangleq \theta_d$, consequently, we have $e_\theta = \theta - \theta_d = 0$. Therefore, equation (26) can be calculated as follows

$$\frac{k}{(M+m)} \cdot e_E x = 0 \tag{27}$$

By combining equations (5) and (27) and differentiating both sides of equation (27), we have the following

$$\frac{k}{(M+m)} \cdot \left(e_E \dot{x} + \tau_1 \dot{\theta} x\right) = 0 \tag{28}$$

According to equations (21) and (5), and by differentiating both sides of equation (28), we have the following

$$e_E \ddot{x} = 0 \tag{29}$$

By substituting equation (27) into (29), we have the following

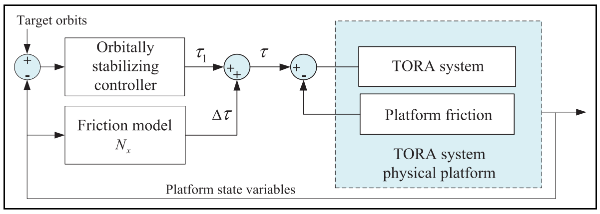

Figure 4. The redesign process of the orbitally stabilizing controller with compensation control.

$$e_E\left(\ddot{x} + \frac{k}{M+m}x\right) = 0 \tag{30}$$

According to equation (7), to solve the above equation, we have the following

$$e_E = \frac{1}{2}k\left(C^2 - x_A^2\right) = 0 \tag{31}$$

and

$$x = C\sin\left(\frac{2\pi}{T}t + \sigma\right) \tag{32}$$

where we define C denoting the amplitude of periodic orbit and σ denoting initial phase in equation (8), that is, $C \triangleq x_A$ and $\sigma \triangleq \varphi$. Then, by differentiating both sides of equation (32), we have the following

$$\dot{x} = x_A \frac{2\pi}{T}\cos\left(\frac{2\pi}{T}t + \varphi\right) = \dot{x}_d(t) \tag{33}$$

Finally, we have $(x, \dot{x}, \theta, \dot{\theta}) = (x_d, \dot{x}_d, \theta_d, 0)$ in $\mathbf{\Gamma}_m$ based on LaSalle's Invariance Theorem. The proposed controller (equation (15)) can drive x, $\dot{x}$, θ, and $\dot{\theta}$ converging to the target orbits.

Friction compensation control

For TORA system, it is straightforward to see that the proposed controller τ_1, that is, equation (15), has good control performance to force the translational cart to oscillate periodically and the actuator to track the desired orbit. However, it can be hardly applied to the physical platform, which always exists kinetic friction negatively influencing orbitally stabilizing control.

In TORA platform, with the translational cart oscillating periodically, the matched external frictional effects are unavoidably encountered, which would lead to mission failure such as giving rise to unstable results. For this, a simple feedforward control with consideration for frictional compensation is added to keep the performance of proposed orbitally stabilizing controller.

As shown in Figure 4, let $\Delta\tau$ denote the compensation control torque and it is straightforwardly to see

$$\tau = \tau_1 + \Delta\tau \tag{34}$$

where τ dentes control input torque applied to the TORA platform. According to the TORA dynamics (equations (1), (2), and (34)), we have the following

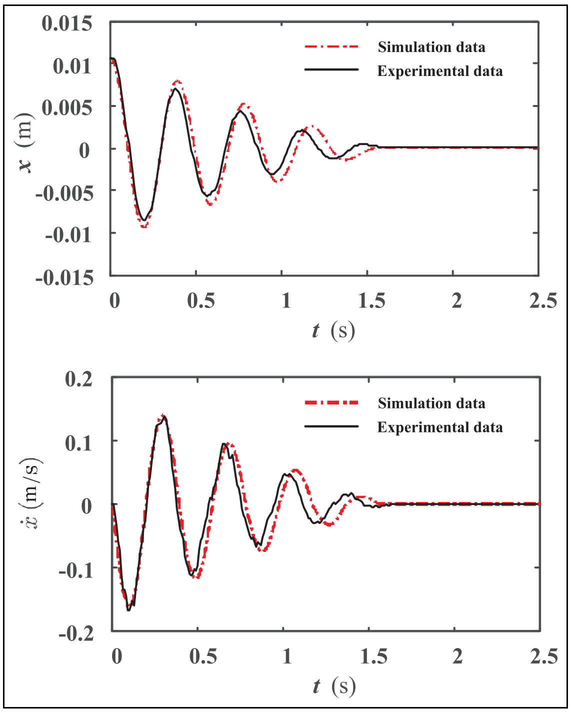

Figure 5. The position and velocity of the translational cart in free oscillation; initial TORA conditions are chosen as $[x, \dot{x}, \theta, \dot{\theta}, \tau]^T|_{(t=0)} = [0.0107, 0, \pi/2, 0, 0]^T$ (black solid line: experimental data based on TORA platform; red dashed line: simulation data based on TORA dynamics).

$$\ddot{x} = -f(\cdot)\tau_1 - g(\cdot)h_1 - \frac{mr\cos\theta\Delta\tau + (mr^2 + I)N_x}{\Omega} \tag{35}$$

where $f(\cdot) = mr\cos\theta/\Omega$ and $g(\cdot) = mr^2 + I/\Omega$. To compensate N_x, let $mr\cos\theta\Delta\tau + (mr^2 + I)N_x = 0$, we have the following

$$\Delta\tau = -\frac{mr^2 + I}{mr\cos\theta}N_x \tag{36}$$

Substituting equations (15) and (36) into equation (34), physical control input torque τ applied to the TORA platform can be calculated as follows

$$\tau = -\frac{\Omega(k_4\dot{\theta} + k_2 e_\theta) + k_3 mrh_1\cos\theta}{k_1 e_E\Omega + k_3(M+m)} - \frac{mr^2 + I}{mr\cos\theta}N_x \tag{37}$$

Remark 4. Note that the angular positions $n\pi$ are the transient singularities of the compensation control torque in equation (36). In practice, $\Delta\tau$ can drive θ pass through the positions as $n\pi$ quickly to avoid the transient singularities. Hence, if the target orbit of eccentric rotational actuator is selected as $\theta_d = n\pi$, θ can be dynamically stabilized near the θ_d.

Remark 5. Comparing the construction of two controllers (equations (15) and (37)), $\Delta\tau$ is the key difference which can be regarded as the continuous excitation source of the translational and rotational movements. Hence, $\Delta\tau$ plays the role of position feedback in an alternative way. For the controller (equation (37)), as long as θ and $\dot{\theta}$ are nonzero, they will continually cause the oscillations of translational cart due to the inherent coupling interaction. Based on this, by self-sustaining rotational motions of the actuator, the cart can track its target orbit and not be stabilized even for the existence of translational friction, which is actually inevitable.

The following step is the definition of a suitable friction model and the identification of the relative parameters. Based on the complicated estimates methods proposed by Pavlov et al.[4] and Lee and Chang,[5] the cart in TORA system moves with changes in its translational velocity $\dot{x}$, and the identified kinetic friction is obtained from the variation in cart velocity $\dot{x}$. Then, we simplify a suitable friction model for the TORA platform as follows

$$N_x = \mu_1(M + m)g \cdot \mathrm{sgn}(\dot{x}) + \mu_2\dot{x} \tag{38}$$

where μ_1 denotes the coulomb frictional coefficient, and μ_2 denotes the viscous frictional coefficient.

Without control torque acting, in the initial TORA conditions such as $[x, \dot{x}, \theta, \dot{\theta}, \tau]^T|_{(t=0)} = [0.0107, 0, \pi/2, 0, 0]^T$, the TORA platform can be degraded to a simple mass–spring system, whose free oscillation phenomenon will finally disappear. Based on this, the friction model N_x can be identified through the outputs coming from the free oscillation of the translational cart. As shown in Figure 5, the outputs, that is, x or $\dot{x}$, coming from simulation data and experimental data can fit well each other within 0.5 s. Consequently, it can be concluded that μ_1 is 0.017 and μ_2 is 0.5 in equation (38). After 0.5 s, the outputs x or $\dot{x}$ cannot fit well for the phase deviation, which could be hardly neglected once the amplitude of the translational cart is near equilibrium point. To avoid phase deviation, choose enough large amplitude of the target orbit such as 0.008 m, which can hold the precision of the proposed friction model N_x.

Simulations and experiments

In the section, based on simulations, we first make the performance comparison between τ_1 and τ, that is, the orbitally stabilizing controller (equation (15)) and physical control input torque (equation (37)), to verify the validity of the compensation control design. After that, both simulation and experimental results are included to verify the validity of physical control input torque (equation (37)) applied to the TORA platform.

To make the performance comparison between τ_1 and τ, in the following simulation works, first, the given physical parameters and initial conditions keep same as the TORA platform (see Figure 7). Then, the target periodic orbits are chosen as $x_d(t) = 0.008\sin(16.11t - 0.65\pi)$, $\theta_d = 2\pi$. Finally, the

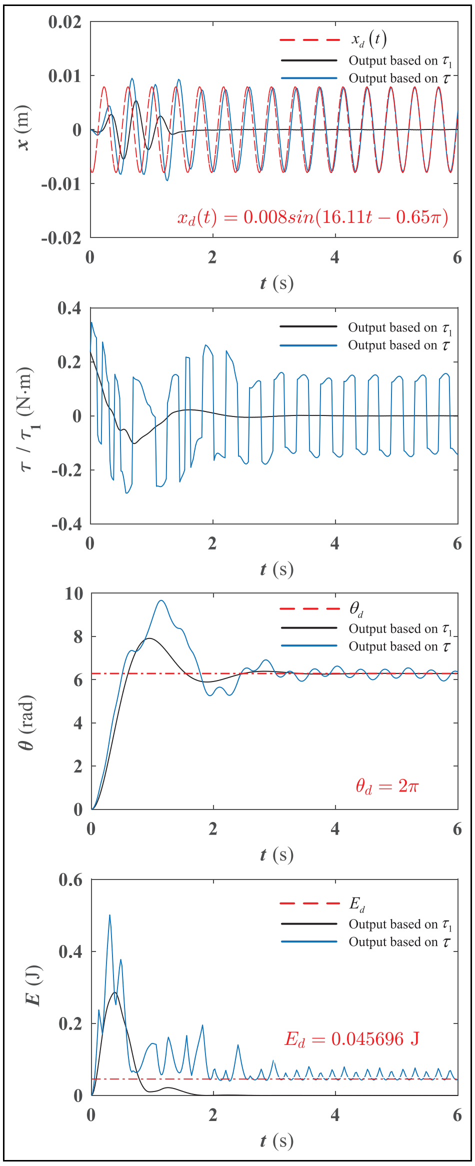

Figure 6. The performance comparison between τ_1 and τ based on simulations; target orbits are chosen as $x_d(t) = 0.008 \sin(16.11t - 0.65\pi)$, $\theta_d = 2\pi$.

control parameters in (equation (37)) are tuned as $k_1 = 1$, $k_2 = 10.2$, $k_3 = 0.78$, $k_4 = 2.25$.

Figure 6 shows the different state outputs comparison based on τ_1 and τ. For the outputs based on the orbitally stabilizing controller τ_1, with the energy dissipation caused by kinetic friction, the translational cart cannot maintain the self-sustained oscillations and then achieves static equilibrium within 2 s. Meanwhile, the total energy E is reduced rapidly to zero within 2 s. After that, the eccentric rotational actuator would stabilize at at 2π. In comparison, the performance of physical control input torque τ is better to track both target periodic orbits. The translational cart can realize target periodic oscillation after 4 s, and the total energy E dynamically stabilizes at E_d after 4 s. The angular position θ will be fluctuated around 2π. This phenomenon is synchronously caused by the compensation control

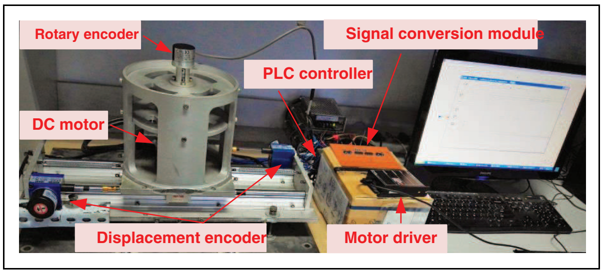

Figure 7. The outline of TORA system platform.

torque $\Delta\tau$. Furthermore, note that the value of physical control input torque τ is not more than ± 0.4 N m, which is needed to input with time varying for overcoming the negative influence of kinetic friction.

The following is to verify the validity of physical control input torque (equation (37)) applied to the TORA platform, which is shown in Figure 7. In experimental works on TORA platform, the details including the physical parameters, initial conditions, the target periodic orbits, and the control parameters are the same in the above simulation works.

For the TORA platform, actuated by the DC servo motor, the eccentric rotational actuator rotates around the center of the motor axle. The position of translational cart is collected in real time by the incremental optical encoder (1024 p/10 mm). The angular position of the actuator is collected in real time by the angular encoder (4096 PPR) attached to the top of the DC servo motor. The physical constraints of the DC servo motor in equation (37) are artificially set as follows

$$|\tau| \leqslant 0.496 \text{ N m} \tag{39}$$

The programmable logic controller (PLC; Siemens S7-200) is used to read sensor feedback signals and convey them to graphical user interface (GUI) in the host PC; meanwhile, it also outputs the calculated control orders to the DC servo motor to control the movements of the cart and the actuator, so that the real-time control task can be accomplished. Moreover, the sampling period of the PLC is 20 ms.

Figure 8 shows the experimental results of the proposed physical control input torque (equation (37)) applied to the TORA platform. According to the experimental results, there are phase deviations in the curves of x, τ, θ, and E by comparison the simulation results before 2.5 s because the response time leads to control delay in real applications. After 2.5 s, the experimental curves of x, τ, θ, and E are in good accordance with their simulation curves. Moreover, the translational cart oscillates along x-direction and the oscillation center is the equilibrium point, and the periodic oscillation amplitude of translational cart is 0.008 m because the total system energy is compensated after 2.5 s. Note that both the simulation and experimental orbit curves of the translational cart are not absolute sine curves. One reason is that the nonlinear

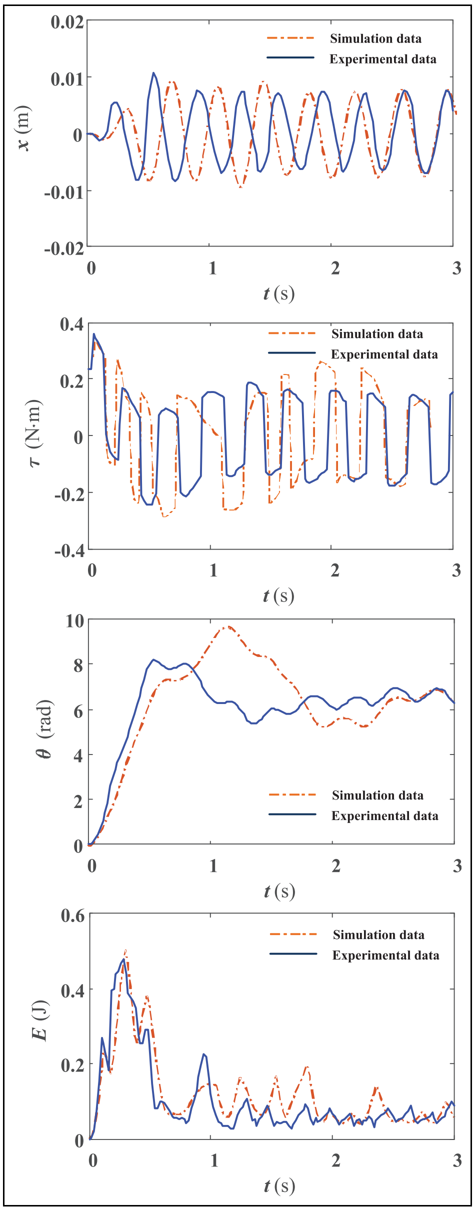

Figure 8. Experimental results of the physical control input torque τ on TORA platform; target orbits are chosen as $x_d(t) = 0.008\sin(16.11t - 0.65\pi)$, $\theta_d = 2\pi$.

coupling interaction coming from the oscillating motion of the cart can act on the actuator, which influences on oscillating period of the cart. The other reason is that the control errors is always produced by unmodeled dynamics of the actuator in TORA platform and disturbances.

Conclusion

Orbitally stabilizing control of the UMS is interesting and challengeable. This article presents the novel periodic orbits and a concise orbitally stabilizing control design for the underactuated TORA system. The design of target periodic orbits assumed that the translational oscillation cart oscillating periodically, while the eccentric rotational actuator is stabilized at the fixed angle. The orbitally stabilizing control extends the traditional control objective of TORA system in comparison with its stabilizing control of equilibrium points. A proper control Lyapunov function including system energy is designed to obtain orbitally stabilizing controller. The asymptotic stability of the closed-loop orbitally stabilizing controller is proved based on LaSalle's Invariance Theorem. Simulations and experiments are performed with consideration for friction compensation to demonstrate the availability of the presented orbitally stabilizing controller applied to the TORA platform.

In future work, the orbitally stabilizing control design will be applied to determine the scope of the possible target periodic orbits with different motor drive capabilities and friction conditions. Moreover, the closed-loop compensation control based on different periodic orbits will be further characterized to maintain the stability of the TORA system.

Declaration of conflicting interests

The author(s) declared no potential conflicts of interest with respect to the research, authorship, and/or publication of this article.

Funding

The author(s) disclosed receipt of the following financial support for the research, authorship, and/or publication of this article: This research project was supported in part by Jiangsu Province "Six Big Talent Peak Program" (2014-ZBZZ-001) and in part by the Outstanding Young Teacher in Southeast University (2242015 R30024).

References

1. Sun N, Wu YM, Fang YC, et al. Nonlinear antiswing control for crane systems with double-pendulum swing effects and uncertain parameters: design and experiments. *IEEE T Autom Sci Eng* 2018; 15: 1413–1422.
2. Bupp RT, Bernstein DS and Coppola VT. A benchmark problem for nonlinear control design. *Int J Robust Nonlin* 1998; 8: 307–310.
3. Park P and Choi DJ. LPV controller design for the nonlinear RTAC system. *Int J Robust Nonlin* 2001; 11(14): 1343–1363.
4. Pavlov A, Janssen B, van de Wouw N, et al. Experimental output regulation for a nonlinear benchmark system. *IEEE T Contr Syst T* 2007; 15(4): 786–793.
5. Lee CH and Chang SK. Experimental implementation of nonlinear TORA system and adaptive backstepping controller design. *Neural Comput Appl* 2012; 21(4): 785–800.
6. Gao BT, Xu J, Zhao JG, et al. Stabilizing control of an underactuated 2-dimensional TORA with only rotor angle measurement. *Asian J Control* 2013; 15(3): 1477–1488.
7. Fabio C. Output regulation for the TORA benchmark via rotational position feedback. *Automatica* 2011; 47(3): 584–590.

8. Sun N, Wu YM, Fang YC, et al. Nonlinear continuous global stabilization control for underactuated RTAC systems: design, analysis, and experimentation. *IEEE/ASME T Mech* 2017; 22(2): 1104–1115.
9. Shiriaev A, Ludvigsen H, Egeland O, et al. On global properties of passivity based control of the inverted pendulum. *Int J Robust Nonlin* 1999; 3: 2513–2518.
10. Nakanishi J, Member S, Fukuda T, et al. A brachiating robot controller. *IEEE T Robotic Autom* 2000; 16(2): 109–123.
11. Xin X and Liu YN. Reduced-order stable controllers for twolink underactuated planar robots. *Automatica* 2013; 49(7): 2176–2183.
12. Xia DY, Wang LY and Chai TY. Neural-network-friction compensation-based energy swing-up control of Pendubot. *IEEE T Ind Electron* 2014; 61(3): 1411–1423.
13. Zhao JG, Zhao TY, Xi N, et al. MSU Tailbot: controlling aerial maneuver of a miniature-tailed jumping robot. *IEEE/ASME T Mech* 2015; 20(6): 2903–2914.
14. Soto MG and Adeli H. Tuned mass dampers. *Arch Comput Method E* 2013; 20(4): 419–431.
15. He XM and Liu CS. Dynamics and screening characteristics of a vibrating screen with variable elliptical trace. *Min Sci Technol* 2009; 19(4): 508–513.
16. Sloot E and Kruyt NP. Theoretical and experimental study of the transport of granular materials by inclined vibratory conveyors. *Powder Technol* 1996; 87(3): 203–210.
17. Korkmaz O, Ider SK and Ozgoren MK. Trajectory tracking control of an underactuated underwater vehicle redundant manipulator system. *Asian J Control* 2016; 18(5): 1593–1607.
18. Islam S, Liu PX and Saddik AE. Nonlinear robust adaptive sliding mode control design for miniature unmanned multirotor aerial vehicle. *Int J Control Autom* 2017; 15(10): 1661–1668.
19. Zhang AC, She JH, Lai XZ, et al. Motion planning and tracking control for an acrobot based on a rewinding approach. *Automatica* 2013; 49(1): 278–284.
20. Quan Q and Cai KY. Additive-state-decomposition-based tracking control for TORA benchmark. *J Sound Vib* 2013; 332(20): 4829–4841.
21. Chung CC and Hauser J. Nonlinear control of a swinging pendulum. *Automatica* 1995; 31(6): 851–862.
22. Shiriaev A, Perram JW and Canudas-de-Wit C. Constructive tool for orbital stabilization of underactuated nonlinear systems: virtual constraints approach. *IEEE T Automat Contr* 2005; 50(8): 1164–1176.
23. John G, Alberto O and Ernesto S. Energy-optimal trajectory planning for the Pendubot and the Acrobot. *Optim Contr Appl Met* 2013; 34(3): 275–295.
24. Gao BT, Liu CD and Cheng HT. Virtual constraints based control design of an inclined translational oscillator with rotational actuator system. *Shock Vib* 2015; 2015: 769151.
25. Li ZF, Tong X, Zhou B, et al. Modeling and parameter optimization for the design of vibrating screens. *Miner Eng* 2015; 83: 149–155.
26. Jiang HS, Zhao YM, Duan CL, et al. Kinematics of variableamplitude screen and analysis of particle behavior during the process of coal screening. *Powder Technol* 2017; 306: 88–95.
27. Isidori A. *Nonlinear control systems*. Boston, MA: Springer Science & Business Media, 2013.